

Free charge carriers in mesoporous silicon

V. Yu. Timoshenko,^{1,2} Th. Dittrich,¹ V. Lysenko,³ M. G. Lisachenko,² and F. Koch¹¹Technische Universität München, Physik Department E16, D-85748 Garching, Germany²M. V. Lomonosov Moscow State University, Physics Department, 119899 Moscow, Russia³INSA de Lyon, LPM, 20 av. Albert Einstein, Bat. 502, 69621 Villeurbanne Cedex, France

(Received 14 December 2000; revised manuscript received 19 March 2001; published 7 August 2001)

Free charge carriers in mesoporous Si (meso-PS) consisting of Si nanocrystals of small dimensions of about 6–10 nm are investigated by the infrared-absorption technique. Adsorption of acceptor molecules or filling the pores with dielectric liquids are found to increase the concentration of free holes (p) in meso-PS up to the half of the doping level of the heavily boron-doped p^+ -Si substrate ($p \sim 5 \times 10^{18} \text{ cm}^{-3}$) from which the meso-PS was made. Considering the value of p and the dc electrical conductivity σ , the hole mobility is determined as about 5×10^{-4} and $5 \times 10^{-3} \text{ cm}^2 \text{ V}^{-1} \text{ s}^{-1}$ for as-prepared meso-PS and meso-PS filled with a polar dielectric liquid, respectively. The activation energy is larger for σ than for p giving evidence for thermal activation of the hole mobility. A model of the dielectric confinement for charge carriers and hydrogenic impurities is applied to explain the dependence of σ and p on the dielectric constant of the ambience of the Si nanocrystals.

DOI: 10.1103/PhysRevB.64.085314

PACS number(s): 68.08.-p, 82.45.-h, 81.65.-b

I. INTRODUCTION

The existence of free charge carriers in porous semiconductors or semiconductor nanocrystals is a complex problem, which concerns questions as carrier localization, compensation, and binding energy of charge carriers in nanocrystals with a dielectrically modified ambience. The importance of the dielectric confinement for the binding energy of hydrogenic impurities and excitons in semiconductor nanostructures was discussed for the first time by Keldysh.¹ However, the experimental proof of the pure dielectric confinement, i.e., the dependence of the free-carrier concentration on the dielectric constant of the ambience of the semiconductor nanocrystal is complicated due to the complexity of the problem. Mesoporous silicon (meso-PS) may serve as a model system to investigate free charge carriers in porous semiconductors for three main reasons.

(i) Meso-PS consists of interconnected Si nanowires (diameters 6–10 nm).² Such structures are optimal for studying dielectric effects since the quantum confinement does not strongly modify their electronic states.^{3,4}

(ii) Meso-PS is formed from heavily doped p -type Si (p^+ -Si) and the doping impurities are not removed during the electrochemical formation process.^{5,6}

(iii) The huge internal surface (area of the order of $100 \text{ m}^2/\text{cm}^3$) (Ref. 7) can be well passivated for Si surfaces, which gives the opportunity to separate processes related to surface states from those being related to dielectric effects.

The absence of free charge carriers in meso-PS has been suggested in numerous works (see, for example, Refs. 5, 6, 8, and 9) regarding its very low electrical dc conductivity σ . Actually, σ in meso-PS is typically in the range between 10^{-4} and $10^{-7} \Omega^{-1} \text{ cm}^{-1}$, which is much lower than for the p^+ -Si substrate ($\sigma \sim 10^2\text{--}10^3 \Omega^{-1} \text{ cm}^{-1}$).^{9–11} The low value of σ cannot be explained by carrier depletion due to the quantum-confinement effect as for nanoporous Si (nano-PS).^{8,12,13} According to Lehmann *et al.*¹⁰ the low value of σ in meso-PS is caused by charged-surface traps constricting conductive pathways in the silicon skeleton by Coulomb

repulsion. Other interpretations of the low value of σ are based on hypotheses of hydrogen passivation of doping impurities inside the Si nanocrystallites,⁹ of location of doping atoms at the surface of the nanowires,⁶ or of complete compensation by surface states.⁸

The concentration (free-hole concentration p) and mobility μ of free carriers determine the value of σ . A low value of μ was estimated from ambipolar diffusion measurements in meso-PS ($10^{-4}\text{--}10^{-5} \text{ cm}^2 \text{ V}^{-1} \text{ s}^{-1}$) (Ref. 11) and excludes the argument of full compensation ($p \approx 10^{10} \text{ cm}^{-3}$). Convincing data of p are practically not available for meso-PS. There is only one publication giving values for the free-electron concentration and Hall mobility in meso-PS formed from heavily doped n -type Si.¹⁴ But these results cannot be applied to conventional meso-PS formed from p^+ -Si due to very different morphology and sizes of the Si nanostructures.¹⁵

The measurement of the free-carrier concentration by infrared (IR) spectroscopy is a standard method for bulk semiconductors. It can be also applied to meso-PS if taking into account that the length of interaction of free charge carriers with electromagnetic waves of the middle IR range is of the order of 1 nm, i.e., much lower than the characteristic dimensions of the interconnected Si nanowires. The IR absorption by free carriers is a second-order process,¹⁶ the contribution of which should be detected as a background of the IR absorption by chemical bonds at the huge internal surface. Thei β ¹⁷ simulated the IR reflectance spectrum of meso-PS formed from strongly degenerated p^+ -Si ($p = 1.1 \times 10^{20} \text{ cm}^{-3}$) using the Drude model and a reduced p of $2.3 \times 10^{18} \text{ cm}^{-3}$. Direct evidence of the IR free-carrier absorption in meso-PS has been recently reported.¹⁸

The electronic properties of porous silicon are very sensitive to different gases^{19–22} and polar liquids.^{20,23,24} Various mechanisms of adsorption-induced modification of the photoluminescence of nano-PS were reported^{24–26} and the influence of polar liquids on excitonic states in Si nanocrystals was shown by the anticorrelation of the photoluminescence efficiency and dielectric function of polar liquid.^{25,26} One

should expect a similar influence of the dielectric ambient on the impurity binding energy in meso-PS as on the exciton binding energy in nano-PS due to the similarity of the electrostatic problem for an exciton and an impurity atom inside Si nanocrystals. On the other hand, adsorbed or condensed molecules change the electronic states at the internal surface of meso-PS. For example, a strong increase of σ in meso-PS was observed after absorption of NO_2 (electron-acceptor) molecules,²² which can be related to the strong increase of p .¹⁸

The current paper is aimed at determining the concentration of free carriers in meso-PS and to show the role of different adsorbed and condensed molecules inside the pores. The effect of dielectric confinement is separated from surface-related effects. The independent investigation of p (infrared free-carrier absorption) and σ (dc electrical conductivity of Au/meso-PS/ p^+ -Si structures) is used to estimate μ in meso-PS under different conditions.

II. EXPERIMENTAL DETAILS

Meso-PS layers were formed from p^+ -Si wafers (100) (boron doped, $\rho \approx 15 \text{ m}\Omega \text{ cm}$) by electrochemical anodization in HF-based solution [HF(48%):ethanol=1:1] at a current density of 50 mA/cm^2 . The free-standing meso-PS films were obtained by lifting during a short electropolishing step at a current density of 500 mA/cm^2 . After fabrication the samples were shortly rinsed in water and dried in N_2 flow. The porosity was about 50%. The thickness d ranged from 10 to $75 \mu\text{m}$ depending on the anodization time. According to analysis of Raman spectra²⁷ the mean diameter of the Si nanocrystals (approximated by a model of cylindrical wires) was about 7–9 nm.

Free-standing meso-PS films were investigated by Fourier transform infrared (FTIR) spectroscopy using a Bomem DA-3 FTIR spectrometer in transmission mode. The measurements were performed in the spectral range from 500 cm^{-1} to 4500 cm^{-1} at different temperatures.

Current-voltage (I - V) measurements were carried out on Au/meso-PS/ p^+ -Si structures. The Au contacts (100 nm thick) were evaporated on meso-PS layers via a mask of 2 mm^2 area. The Ohmic back contact to the p^+ -Si was made by InGa alloy. The I - V characteristics were measured with a HP4140B digital pA meter in a narrow potential range around 0 V to avoid any injection effect. The 30–60 μm thick meso-PS layers were used to eliminate an influence of the Schottky barrier at the Au/meso-PS interface for the determination of σ .²⁸ The I - V measurements were performed in a vacuum chamber in different environments (vacuum, air, vapors of organic liquids) at different temperatures. The dependence of σ on the presence of adsorbed or condensed organic molecules was studied for the organic substances with different static dielectric constants: ethanol, cyclohexane, trichloroethane, and isobutylmethylketon. The condensation of the molecules inside the pores was controlled by the reflectance measurement of meso-PS using a probe beam of a He:Ne laser (633 nm). The reflection coefficient of meso-PS increased when the molecule condensation occurred. According to the reflectance measurements the con-

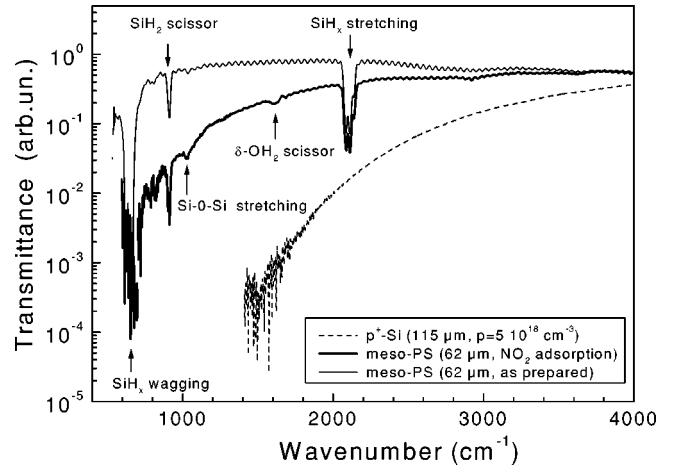


FIG. 1. IR transmittance spectra of a p^+ -Si wafer and as-prepared free-standing meso-PS films in vacuum and after adsorption of NO_2 molecules ($p_{\text{NO}_2} \approx 0.1 \text{ mbar}$).

densation of vapor of the investigated organic liquids in the pores always took place at the vapor pressure $P = P_s$ and was avoided at the partial pressure $P < P_s/5$, where P_s is the saturation pressure of corresponding dielectrics.

III. IR FREE-CARRIER ABSORPTION

A. The concentration of free carriers

Typical IR transmittance (T) spectra are shown in Fig. 1 for as-prepared meso-PS, meso-PS after adsorption of NO_2 molecules, and for the p^+ -Si substrate. The logarithmic scale of T is chosen to show simultaneously both vibrational modes of surface bonds and features related to the IR free-carrier absorption in meso-PS. The Si-H_x stretching modes ($2050\text{--}2200 \text{ cm}^{-1}$), Si-H_2 scissors mode, and Si-H_x wagging modes ($620\text{--}715 \text{ cm}^{-1}$) are dominating and traces of oxides (Si-O-Si stretching modes at $1070\text{--}1190 \text{ cm}^{-1}$) (Ref. 17) are absent in as-prepared meso-PS. Small absorption due to the Si-O-Si and O-H_2 stretching modes appears in meso-PS after adsorption of NO_2 molecules, which can be related to well-known oxidative activity of NO_2 .²⁴ Further, water molecules are able to stick to oxidized Si bonds due to their hydrophilic nature. At the same time, NO_2^- species (vibrational modes at 818 cm^{-1} , 1230 cm^{-1} , and 1340 cm^{-1}) (Ref. 22) are not clearly observed due to their small amount at the meso-PS surface.

The strong decrease of the transmittance of p^+ -Si towards the lower frequency belongs to the IR absorption by free charge carriers (holes). The spectral-dependent background of the transmittance of as-prepared meso-PS (i.e., the spectrum of T excluding contributions of the Fabry-Perot interference and surface-vibrational bands) decreases by ten times in the spectral range from 2000 cm^{-1} to 500 cm^{-1} (see Fig. 1). This continuous decrease of T with decreasing frequency gives evidence for the free-carrier absorption in meso-PS.²⁹ The decrease of T at lower frequencies becomes much more pronounced for meso-PS with adsorbed molecules of NO_2 being acceptors of electrons on semicon-

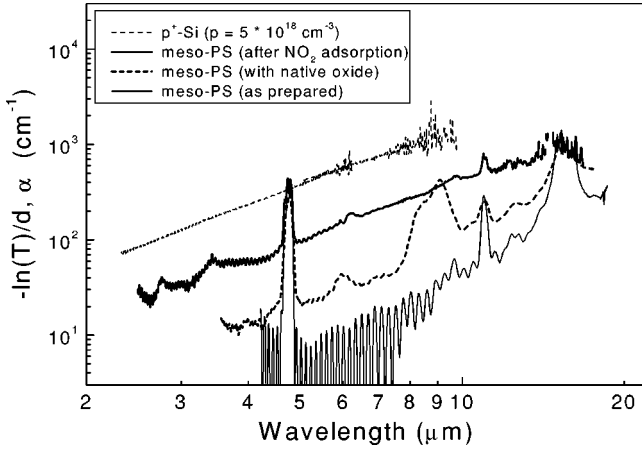


FIG. 2. IR absorption spectra of p^+ -Si substrate and free-standing meso-PS films with different surface treatment.

ductor surfaces.³⁵ This fact demonstrates that the free holes are just responsible for the IR free-carrier absorption in meso-PS and the value of p increases with adsorption of acceptorlike molecules.

The absorption coefficient α should be analyzed in order to determine the value of p in meso-PS. The value of α is proportional to $[-\ln(T)]/d$ if not taking into account the spectral dependence of the reflection coefficient R . R can be obtained for meso-PS if neglecting interference fringes and the contribution of chemical bonds. R of meso-PS is practically constant in the middle-IR spectral range and amounts to 0.15–0.2, which is in good agreement with the effective medium approximation³⁰ (R of bulk Si, 0.3; porosity, 50%). Note, the contribution of free carries to R is more significant for the p^+ -Si sample since the wavelength corresponding to the plasma frequency is about 10 μm for $p=5 \times 10^{18} \text{ cm}^{-3}$. The absorption coefficient of p^+ -Si can be calculated as $\alpha_{\text{Si}} = [\ln(T_1/T_2)]/(d_1 - d_2)$, where T_1 and T_2 are the transmittances for the wafers of thicknesses d_1 and d_2 , respectively. The spectral dependence of $[-\ln(T)]/d$ for meso-PS with differently conditioned surfaces and α_{Si} for p^+ -Si are plotted in Fig. 2. α_{Si} increases with increasing wavelength by the power law with an exponent of 2. Such spectral behavior can be interpreted in the frame of the classical Drude model, which assumes a constant scattering time for free carriers τ . For sufficiently high frequency of IR radiation, namely, $\omega \gg \tau^{-1}$ one gets $\alpha \sim p\lambda^2\tau/\tilde{n}$, where λ is the wavelength of IR radiation in vacuum and \tilde{n} is the refractive index. The quantum description of the IR free-carrier absorption gives exponents of 1.5, 2.5, and 3 for scattering with acoustic phonons, optical phonons, and ionized impurities, respectively.¹⁶ The constant exponent of 2 for the $\alpha_{\text{Si}}(\lambda)$ dependence gives evidences for a superposition of different scattering mechanisms without domination of one of them. Excluding the contributions of the vibrational bands of surface chemical bonds, the absorption spectra of meso-PS are also characterized by the power law with an exponent of about 2. The similarity of the free-carrier absorption mechanism in meso-PS and in p^+ -Si can be understood if taking into account a small dimension where a free hole interacts

with the electric field of the IR radiation for one period of its oscillation. This dimension can be estimated as $L = v_T\lambda/c$, where $v_T = 10^7 \text{ cm/s}$ is the thermal velocity and $c = 3 \times 10^{10} \text{ cm/s}$ is the speed of light. For $\lambda = 3 - 10 \mu\text{m}$ one gets $L = 1 - 3 \text{ nm}$, which is smaller than the size of nanocrystals in the meso-PS investigated. In this case, surface scattering is not significant for the free-carrier absorption. From the Drude model viewpoint it means that the value of τ in meso-PS is close to that in p^+ -Si. Note, τ in meso-PS should decrease with decreasing size of the Si nanocrystal because the role of surface scattering increases. But the shortening of τ may not be dramatic (about 2.5 times shorter than τ for the substrate) even for the nanocrystals of 3 nm diameter.¹⁷ Therefore the value of τ in meso-PS cannot be used to characterize its dc mobility, which is strongly suppressed comparing with the substrate.¹¹

The value of p in Si nanocrystals of the meso-PS layer can be estimated from the comparison of its α with α_{Si} of the p^+ -Si substrate at a given wavelength. Assuming meso-PS as an effective medium and following the Drude model, the absorption coefficient of the meso-PS layer $\alpha \sim pf\lambda^2\tau/\tilde{n}$, where f is the fill factor (i.e., $f = 1 - r$, where r is the porosity) and \tilde{n} is the refractive index. The value of \tilde{n} is 3.4 for c -Si and about 2.1 (effective medium approximation for $f = 0.5$) (Ref. 30) or 1.8–2.0 (analysis of interference fringes) for as-prepared meso-PS. According to the data shown in Fig. 2 one can obtain $p = 6 \times 10^{16} \text{ cm}^{-3}$ for as-prepared meso-PS. The value of p increases to $(2 - 4) \times 10^{17} \text{ cm}^{-3}$ for the sample with native oxide. The free-carrier concentration is about $(1 - 2) \times 10^{18} \text{ cm}^{-3}$ for the as-prepared meso-PS with adsorbed NO_2 molecules. There may be two possible reasons for different values of p in meso-PS: (i) influence of surface states and (ii) increase of the binding energy of boron acceptors.

B. On the role of surface states

The density of surface states near midgap (D_{it}) at hydrogenated Si surfaces ranges between 10^{10} and $10^{12} \text{ eV}^{-1} \text{ cm}^{-2}$ depending on the kind of hydrogenation.³¹ For example, the lowest values of D_{it} were reached on electrochemically hydrogenated Si surfaces.³² The density of surface states determines the concentration of defects in meso-PS (range of $10^{16} - 10^{18} \text{ cm}^{-3}$). The surface states may have, with respect to their origin, donorlike or acceptorlike or amphoteric character. Amphoteric defects are usually related to Si dangling bonds at intrinsically backbonded Si atoms, which dominate at the Si/SiO₂ interface³³ or in the bulk of hydrogenated amorphous silicon.³⁴ A high concentration of amphoteric surface states will pin the Fermi level of meso-PS near midgap, and free-carrier IR absorption will be absent in this case. Donorlike surface states will trap holes from the Si nanocrystallites and p will be low.

The value of p is quite low in as-prepared meso-PS. This is not surprising since donorlike states are dominating at hydrogenated silicon surfaces.³¹ The concentration of donorlike surface states is relatively high and the low value of p points to trapping of holes at surface states. The origin of the donorlike states at hydrogenated Si surfaces has been related to

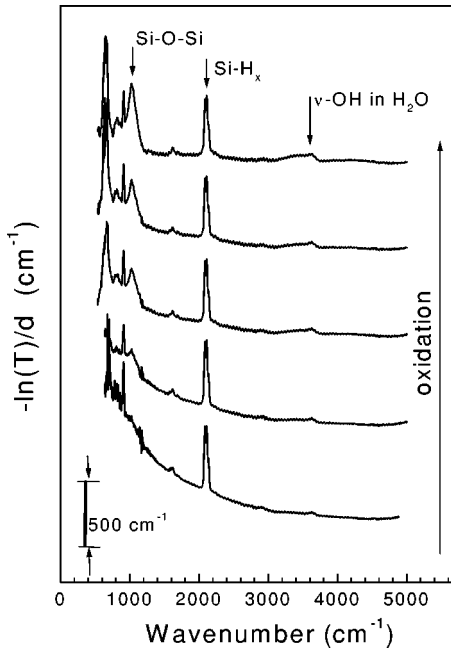


FIG. 3. IR absorption spectra of free-standing meso-PS after adsorption of NO_2 molecules ($p_{\text{NO}_2} \approx 0.1$ mbars) following oxidation in atmosphere of wet oxygen (3 mbars). The arrows mark some vibrational modes.

water molecules (water molecules are donorlike³⁵), which are adsorbed at surface defects.³¹

Molecules of NO_2 act as strong acceptors of electrons at semiconductor surfaces.³⁵ As shown above, the value of p increases dramatically after adsorption of NO_2 molecules on as-prepared meso-PS. We relate the effect of NO_2 molecule on p mostly to the activation of the originally present boron impurities, due to destruction of the bound states of holes at boron acceptors by the electric fields of NO_2^- radicals on surfaces of Si nanocrystals. The strength of the electric field of the NO_2^- radical can be estimated by $q/\epsilon_{\text{eff}}d^2$ as $\sim 10^5$ V/cm for $d=7$ nm and $\epsilon_{\text{eff}}=4.5$. Such strong electric fields can ionize boron impurities in Si nanocrystals and p will reach the doping level of the p^+ -Si substrate. The ionization mechanism is a tunneling through a barrier reduced by the electric field of the NO_2^- radical. This ionization mechanism is similar to the Zener-effect for p - n junctions.^{16,36} The other possibility, i.e., doping of the meso-PS by adsorbed NO_2 molecules itself, cannot be ruled out. But, one should keep in mind that the tremendous increase of σ (Ref. 22) and p (our experiments) due to adsorption of NO_2 molecules is observed only for meso-PS but not for nano-PS formed on slightly doped p -Si. Therefore, the formation of NO_2^- radicals does not necessarily lead to the generation of free holes.

In order to demonstrate the role of surface states, the as-prepared samples with adsorbed NO_2 molecules were oxidized in wet atmosphere at low pressure. The results of the FTIR measurements are presented in Fig. 3. The absorption by free carriers decreases with the development of the oxidation process (growth of the Si-O-Si absorption band), and the IR absorption bands of physisorbed water molecules

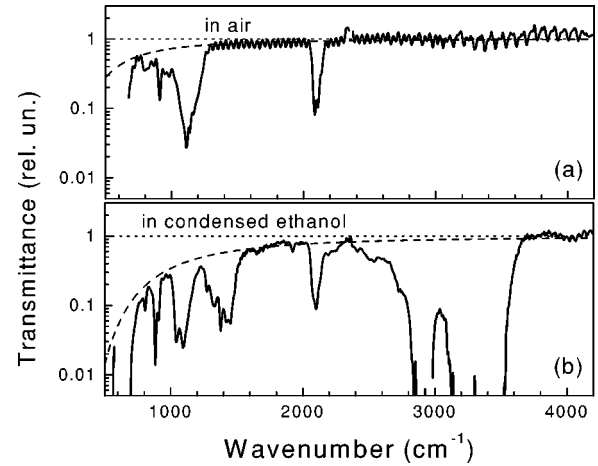


FIG. 4. IR transmittance spectra of free-standing meso-PS film in air (a) and in condensed ethanol vapors (b). The dashed lines fit the backgrounds of the spectra for Drude-like free-carrier absorption with $p=10^{17}$ cm^{-3} (a) and $p=3 \times 10^{18}$ cm^{-3} (b).

(broad OH stretching mode around 3500 cm^{-1} , OH_2 scissor mode at 1650 cm^{-1}) becomes more pronounced. The strong decrease of p with ongoing initial oxidation is caused by increasing the concentration of adsorbed water molecules and/or by the development of surface states acting as compensating defects. We remark that the concentrations of the different surface states depend sensitively on the procedure of oxidation. Therefore, the values of p can be quite different for slightly oxidized meso-PS under different experimental conditions.

C. Effect of dielectric ambience

The effect of dielectric ambience for the free-carrier concentration in Si nanocrystals was examined by filling of the pores in meso-PS with ethanol. The latter was chosen because liquid ethanol has a large dielectric constant of $\epsilon_d=25$ and its condensation in the pores increases significantly the effective dielectric constant ϵ_{eff} of meso-PS. Another important peculiarity of ethanol molecules is their relatively weak IR absorption in the spectral range of 500 – 2000 cm^{-1} in comparison to many other polar organic liquids. Figure 4 shows the IR transmittance spectra for the natively oxidized meso-PS film in air (a) and in condensed ethanol (b). It is important to note that the effect of the ethanol condensation on the transmittance was reversible for many filling-drying cycles. The ethanol condensation leads to a strong decrease of the IR transmittance at the lower frequencies. We point out that adsorption of ethanol molecules at a semiconductor surface leads to the creation of donorlike surface states,³⁵ which should reduce the free-hole concentration in p -type Si. But the strong increase of p in the meso-PS after condensation of ethanol shows the importance of the dielectric effect for the activation of boron acceptors in meso-PS. The dashed lines in Fig. 4 fit the background of the spectra of T according to the Drude model of free-carrier absorption. From the model, the free-hole concentration in the meso-PS in air is about 10^{17} cm^{-3} while the sample with condensed

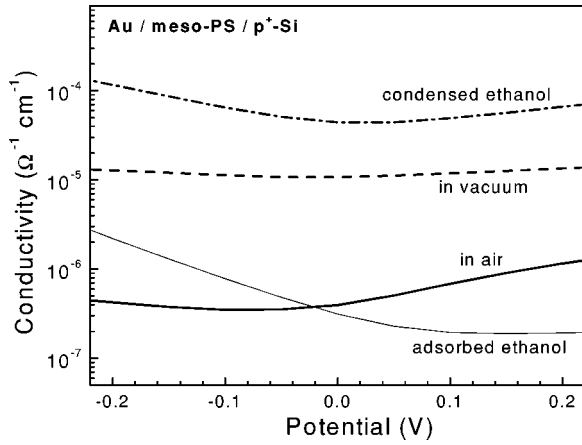


FIG. 5. DC electrical conductivity of Au/meso-PS/ p^+ -Si structure in different ambience.

ethanol is characterized by $p \sim 10^{18} \text{ cm}^{-3}$. A more accurate determination of p in meso-PS after ethanol condensation is complicated by the contribution of the absorption bands of ethanol molecules in the pores.

IV. DC CONDUCTIVITY

Figure 5 shows typical conductivity-voltage characteristics for the Au/meso-PS/ p^+ -Si structures in different ambiences. Injection- or ionization-related phenomena can be neglected for these measurements, which were carried out at very small applied voltage (electric field smaller than 10^2 V/cm). It should be noted that the measurements of σ at large applied voltage, when the electric field in meso-PS was larger than 10^4 V/cm , did not distinguish between the effects of adsorption and condensation of polar molecules in meso-PS.²⁰ The value of σ is $(4-5) \times 10^{-7} \Omega^{-1} \text{ cm}^{-1}$ and about $10^{-5} \Omega^{-1} \text{ cm}^{-1}$ for meso-PS in air and in vacuum, respectively. The pronounced increase of σ for the evacuated meso-PS can be explained by a decreasing density of compensating surface defects related to adsorbed water molecules. The value of μ (so-called dc hole mobility) in as-prepared meso-PS is about $5 \times 10^{-4} \text{ cm}^2 \text{ V}^{-1} \text{ s}^{-1}$ with respect to the values of p and σ . This value is much lower than the hole mobility in crystalline Si but close to the hole drift mobility, which was measured recently in nano-PS by the time-of-flight technique.³⁷

The temperature dependence of σ is plotted in Fig. 6. The conductivity is thermally activated with the activation energy of $E_A = 0.3 \text{ eV}$. This value of E_A is noticeably smaller than that reported for meso-PS in air²¹ and for nano-PS ($E_A = 0.5 \text{ eV}$) (Ref. 8) and demonstrates that the Fermi level can be shifted towards the valence band in meso-PS. The values of p obtained for a small temperature range by FTIR measurements are also plotted in Fig. 6 for the free-standing meso-PS in vacuum. The activation energy of p is about 0.1 eV , which is much smaller than E_A for σ . This points to a thermally activated mobility with E_A about 0.2 eV . We remark, that the activation energy of the hole drift mobility in nano-PS of low porosity is estimated to be $\sim 0.2-0.25 \text{ eV}$.³⁷

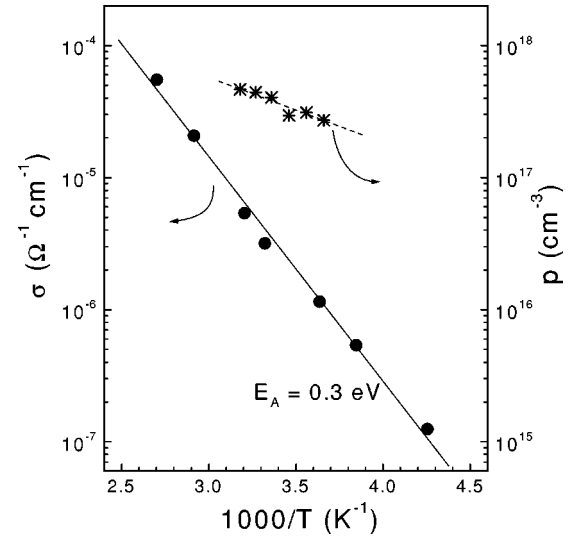


FIG. 6. Arrhenius plot of the dc electrical conductivity of Au/meso-PS/ p^+ -Si structure (circles) in vacuum. The free-hole concentrations (stars) are evaluated from the IR transmittance spectra of free-standing meso-PS film.

The role of surface states for the change of σ after filling the pores of meso-PS with a dielectric liquid can be minimized if comparing the values of the dc electric conductivity with adsorbed (σ_0) or condensed dielectric molecules (σ). The difference between σ_0 and σ is demonstrated in Fig. 5 for adsorbed and condensed ethanol. The electrical conductivity increases strongly after condensation of ethanol inside the pores. Similar results on the increase of the electrical conductivity of meso-PS in the ambience with a large dielectric constant were also obtained for other polar liquids: cyclohexane ($\epsilon_d = 2.0$), trichloroethane ($\epsilon_d = 3.4$), and isobutylmethylketon ($\epsilon_d = 13.1$). The respective dependence for the ratio of σ/σ_0 is shown in Fig. 7 (solid circles). The error bars correspond to the measurements on different samples. The ratio σ/σ_0 increases monotonically with ϵ_d . This fact can be only understood if considering an increase of p or/and μ in meso-PS after filling the pores with a dielectric liquid.

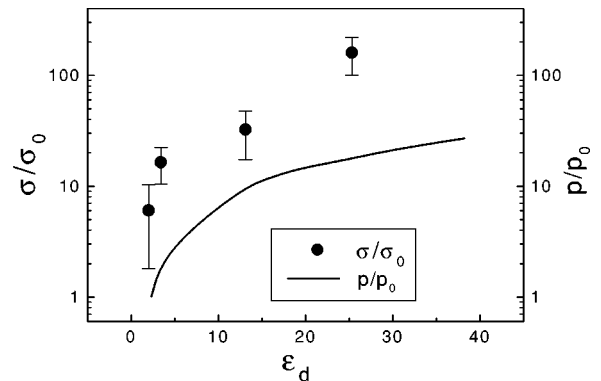


FIG. 7. Dependences of the normalized dc conductivity of meso-PS with condensed molecules of dielectrics (circles) and the calculated changes of the free-hole concentration (line) on the ambient dielectric constant.

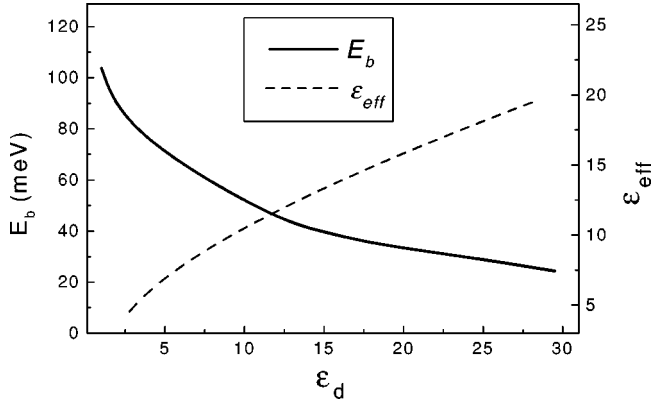


FIG. 8. Calculated binding energy of a boron acceptor (solid line) in a cylindrical Si wire with diameter of 7 nm and effective dielectric constant of the meso-PS of 50% porosity (dashed line) versus the ambient dielectric constant.

V. DIELECTRIC CONFINEMENT IN MESO-PS

The influence of polar liquids on p in meso-PS can be estimated for a hydrogenic-acceptor impurity in the center of a Si nanocrystal. The Si nanocrystal is approximated as an infinite cylinder with diameter $d=7$ nm. Because d is much larger than the Si lattice constant, the dielectric constant inside the cylinder is $\epsilon_S=11.9$ like for bulk Si.¹³ The cylinder is surrounded by a dielectric medium with the effective dielectric constant ϵ_{eff} , which can be calculated using the following expression:³⁰

$$(1-f)(\epsilon_d - \epsilon_{eff})/(\epsilon_d + 2\epsilon_{eff}) + f(\epsilon_S - \epsilon_{eff})/(\epsilon_S + 2\epsilon_{eff}) = 0. \quad (1)$$

The respective dependence of $\epsilon_{eff}(\epsilon_d)$ is plotted in Fig. 8 (dashed line) for the meso-PS of 50% porosity. The value of ϵ_{eff} increases from 4.5 in vacuum or air ($\epsilon_d=1$) to 18 in the ambience of condensed ethanol ($\epsilon_d=25$).

In cylindrical coordinates (z is along the cylinder axis), the potential energy of a hole moving along z axis is given by¹

$$U(z) = -\frac{q^2}{\epsilon_S |z|} - \frac{4q^2(\epsilon_S/\epsilon_{eff} - 1)}{\pi\epsilon_S d} \int_0^\infty \cos(2\xi z) \times \left[\frac{\epsilon_S}{\epsilon_{eff}} \frac{I_1(\xi)}{K_1(\xi)} + \frac{I_0(\xi)}{K_0(\xi)} \right]^{-1} d\xi, \quad (2)$$

where q is elementary charge, $K_{0,1}$ and $I_{0,1}$ are the modified Bessel functions. One can see that the dielectric confinement contributes constructively to $|U(z)|$, when $\epsilon_S > \epsilon_{eff}$, e.g., Si wires in vacuum. But if $\epsilon_S < \epsilon_{eff}$, e.g., Si wires surrounded by polar dielectric liquid, the value $|U(z)|$ will decrease, i.e., the interaction between a charged impurity and a charge carrier will be weaker.

The acceptor binding energy E_b can be calculated by solving the Schrödinger equation with the potential energy given by Eq. (2). The analytical¹ and numerical³⁸ solutions of the problem of a hydrogenic impurity in a semiconductor wire showed strong increase of E_b with decreasing d or/and

increasing $\epsilon_S/\epsilon_{eff}$. For the Si cylindrical wires of 7 nm diameter the calculated dependence of the acceptor binding energy E_b on the dielectric constant of the ambient liquid ϵ_d is shown in Fig. 8 (solid line). The value of E_b decreases from 105 meV to 30 meV when ϵ_d increases from 1 (vacuum) to 25 (ethanol) and $E_b=45$ meV for $\epsilon_d=11.9$ when no mirror charges contribute to $U(z)$. The value of $E_b=105$ meV for $\epsilon_d=1$ is in good agreement with the temperature-dependent FTIR measurements for meso-PS in vacuum (see Fig. 6). It should be noted that for meso-PS filled with condensed polar dielectrics the value of E_b can be influenced by the free-carrier screening, which will additionally decrease E_b than it is shown in Fig. 8.

The values of E_b can be different from those shown in Fig. 8 if an impurity is located far from the axis of a semiconductor cylinder. However the influence of the impurity position on E_b may not be strong because of two effects counteracting each other. On the one hand, the mirror charge effect will be more stronger when the impurity position is far from the cylinder axis.¹ On the other hand, if an impurity is located in the near-surface region of the cylinder, E_b will decrease since the ground state must satisfy the boundary conditions, i.e., be zero on the surface.³⁹ For the surface location of the impurity, its $1s$ state is forbidden while the $2p$ state is allowed and hence E_b will be four times smaller. Simultaneous treatment of these counteracting effects is a complicated theoretical problem. The solution for a hydrogenic impurity located on flat infinite surface of Si crystal gives E_b which is near two times smaller than that for the bulk Si, i.e., the mirror charge effect induces a two times increase of E_b for the $2p$ -ground-state impurity.³⁹ Because of the more important role of the dielectric confinement for semiconductor wires rather than for flat surfaces,¹ one should expect a more significant increase of E_b for the $2p$ -ground-state impurities located on the surface of wire.

The ratio between concentrations of free holes in meso-PS with condensed (p) and adsorbed (p_0) molecules can be obtained as

$$p/p_0 = \exp[(E_{b0} - E_b)/kT], \quad (3)$$

where E_{b0} and E_b are the binding energies for the boron impurities in meso-PS with adsorbed and condensed molecules, respectively. We note, that the expression (3) is valid if the compensation is not strong⁴⁰ and does not significantly differ for meso-PS with adsorbed and condensed molecules. These assumptions are reasonable for our experimental conditions, which is proved by concentrations of free carriers derived from the FTIR data. Thus Eq. (3) can be used to describe both the temperature dependence of p and the effect of dielectric liquids. The p/p_0 ratio calculated according to Eq. (3) for $E_{b0}=105$ meV is plotted as a solid line in Fig. 7. The rise of the ratio σ/σ_0 versus ϵ_d is much stronger than the rise of the calculated ratio of p/p_0 . This difference cannot be simply explained by a size distribution of the nanocrystals typical for meso-PS since $p/p_0=17$ ($\epsilon_d=25$), and the increase of p measured by FTIR for the meso-PS after ethanol condensation (see Fig. 4) is the same within the accuracy of the measurements. Therefore, one should conclude

that μ increases by up to one order of magnitude after filling the pores with a polar liquid. This gives an upper limit of $\mu = 5 \times 10^{-3} \text{ cm}^2 \text{ V}^{-1} \text{ s}^{-1}$.

The low value of μ and its increase after filling of the pores with condensed dielectrics can be understood within the frame of the undulated wire model. The self-image effect due to different ϵ_S and ϵ_d , which is described by the second term in formula (2) induces potential fluctuations for a charge carrier moving in an undulating wire. The self-image contribution to the potential energy of a free hole is roughly proportional to $(\epsilon_S/\epsilon_{eff} - 1)/d$. For instance, a variation of d from 5 to 9 nm along the Si wire kept in a media with $\epsilon_{eff} = 4.5$ (meso-PS in vacuum or in air) will give the modulation of the potential energy of the order of 0.1 eV. Such potential fluctuations would lead to an activation energy of ~ 0.1 eV for μ . The comparison between the temperature-dependent dc conductivity and free-hole concentration allows us to estimate the activation energy of μ to be about 0.2 eV. Note, that even relatively weak quantum confinement (between 20 and 40 meV in each band), which is expected for such wire diameters⁴ can additionally increase the localization of the carriers in undulated wires and thus the activation energy of μ for meso-PS in vacuum. Dielectric medium with $\epsilon_d > \epsilon_S$ surrounding Si wires screens the potential fluctuations related to the self-image effect and therefore μ increases. However the carrier localization due to the quantum confinement may be still present, which together with trapping will limit the carrier transport in meso-PS.

VI. SUMMARY AND CONCLUSIONS

The existence of equilibrium free charge carriers has been shown by free-carrier IR absorption for a porous semiconductor in the case of meso-PS, which was electrochemically produced from heavily boron doped p^+ -Si. The concentration of free holes in meso-PS can be changed over several orders of magnitude up to the order of 10^{18} cm^{-3} by modification of the surface conditioning or by condensation of

dielectric liquids. The free-carrier IR absorption in meso-PS can be described by the Drude-model and the high possible values of p in meso-PS showed that the mechanisms of scattering are comparable for bulk p^+ -Si and meso-PS in the given spectral range.

The specific action of donorlike or acceptorlike or amphoteric surface states has been discussed and the effect of the dielectric ambience on p has been demonstrated. The dielectric confinement is caused by mirror charge, which arises when the dielectric constant of the semiconductor nanoparticle is different from that of its dielectric surrounding ($\epsilon_S \neq \epsilon_d$) and which leads to an increase or decrease of the binding energy of a charge carrier in the Coulomb potential of another one depending on whether $\epsilon_S > \epsilon_d$ or $\epsilon_S < \epsilon_d$, respectively.¹

The simultaneous investigation of the infrared free-carrier absorption and of the dc electric conductivity allowed us to obtain values for the (macroscopic) mobility of free equilibrium holes in meso-PS (of the order of $10^{-4} \text{ cm}^2 \text{ V}^{-1} \text{ s}^{-1}$). We remark that Hall-effect or time-of-flight measurements cannot be applied to this material since the values of the mobility are too small or the conductivity is too big, respectively. It was shown that the mobility is also affected by the dielectric confinement, which is important for the screening of potential fluctuations. However, the generally very small values of the mobility cannot be explained within the model of dielectric confinement and hence, other concepts of the electrical properties of the network of Si nanowires should be considered.

ACKNOWLEDGMENTS

V.Yu.T. is grateful to the Alexander von Humboldt Foundation for support. M.G.L. thanks the Russian Basic Research Foundation (Project No. 99-02-16664) and the Russian Federal Program (Project No. 4.11.99) for financial support.

¹L. V. Keldysh, JETP Lett. **29**, 658 (1979); V. S. Babichenko, L. V. Keldysh, and A. P. Sylin, Fiz. Tverd. Tela (Leningrad) **22**, 723 (1980); L. V. Keldysh, Phys. Status Solidi A **164**, 3 (1997).

²A. G. Cullis, in *Properties of Porous Silicon*, edited by L. Canham (INSPEC, London, 1997), p. 99, and references therein.

³A. J. Read, R. J. Needs, K. J. Nash, L. T. Canham, P. D. J. Calcott, and A. Qteish, Phys. Rev. Lett. **69**, 1232 (1992).

⁴Y. M. Niquet, C. Delerue, G. Allan, and M. Lannoo, Phys. Rev. B **62**, 5109 (2000).

⁵A. Grosman and C. Ortega, in *Properties of Porous Silicon* (Ref. 2), p. 328.

⁶G. Polisski, D. Kovalev, G. G. Dollinger, T. Sulima, and F. Koch, Physica B **273-274**, 951 (1999).

⁷G. Bomchil, A. Halimaoui, and R. Herino, Appl. Surf. Sci. **41/42**, 604 (1989).

⁸M. Ben-Chorin, in *Properties of Porous Silicon* (Ref. 2), p. 165, and references therein.

⁹L. A. Balagurov, D. G. Yarkin, and E. A. Petrova, Mater. Sci. Eng., B **B69-B70**, 127 (2000).

¹⁰V. Lehmann, F. Hofmann, F. Möller, and U. Grüning, Thin Solid Films **255**, 20 (1995).

¹¹R. Schwarz, F. Wang, M. Ben-Chorin, S. Grebner, A. Nikolov, and F. Koch, Thin Solid Films **255**, 23 (1995).

¹²R. Tsu and D. Babic, Appl. Phys. Lett. **64**, 1806 (1994).

¹³M. Lannoo, C. Delerue, and G. Allan, Phys. Rev. Lett. **74**, 3415 (1995).

¹⁴J. Simons, T. I. Cox, M. J. Uren, and P. D. J. Calcott, Thin Solid Films **255**, 12 (1995).

¹⁵A. G. Cullis, L. T. Canham, and P. H. J. Calcott, J. Appl. Phys. **82**, 909 (1997), and references therein.

¹⁶See, for example, K. Seeger, *Semiconductor Physics* (Springer-Verlag, Wien, 1973).

¹⁷W. Theiβ, Thin Solid Films **276**, 7 (1996); W. Theiβ, Surf. Sci. Rep. **29**, 91 (1997).

- ¹⁸V. Yu. Timoshenko, Th. Dittrich, and F. Koch, *Phys. Status Solidi A* **182**, R1 (2000).
- ¹⁹V. M. Demidovich, G. B. Demidovich, E. I. Dobrenkova, and S. N. Kozlov, *Sov. Tech. Phys. Lett.* **18**, 459 (1992).
- ²⁰I. Schechter, M. Ben-Chorin, and A. Kux, *Anal. Chem.* **67**, 3727 (1995).
- ²¹M. Ben-Chorin, A. Kux, and I. Schechter, *Appl. Phys. Lett.* **64**, 481 (1994).
- ²²L. Boarino, C. Baratto, F. Geobaldo, G. Amato, E. Comini, A. M. Rossi, G. Faglia, G. Lerondel, and G. Sberveglieri, *Mater. Sci. Eng., B* **B69-B70**, 210 (2000).
- ²³D. Stievenard and D. Deresmes, *Appl. Phys. Lett.* **67**, 1570 (1995).
- ²⁴M. J. Sailor, in *Properties of Porous Silicon* (Ref. 2), p. 364, and references therein.
- ²⁵E. A. Konstantinova, Th. Dittrich, V. Yu. Timoshenko, and P. K. Kashkarov, *Thin Solid Films* **276**, 265 (1996); P. K. Kashkarov, E. A. Konstantinova, and V. Yu. Timoshenko, *Semiconductors* **30**, 1479 (1996); P. K. Kashkarov, E. A. Konstantinova, A. V. Pavlikov, and V. Yu. Timoshenko, *Phys. Low-Dimens. Struct.* **1-2**, 123 (1997).
- ²⁶S. Fella, R. B. Wehrspohn, N. Gabouse, F. Ozanam, and J.-N. Chazalviel, *J. Lumin.* **80**, 109 (1999).
- ²⁷I. H. Campbell and P. M. Fouchet, *Solid State Commun.* **58**, 739 (1986).
- ²⁸M. Ben-Chorin, F. Möller, and F. Koch, *Phys. Rev. B* **49**, 2981 (1994).
- ²⁹The continuous change of T with wave number is indeed weak for the as-prepared meso-PS and it could be detected in our experiment only for the relatively thick films with $d > 40 \mu\text{m}$.
- ³⁰D. A. G. Bruggeman, *Ann. Phys. (Leipzig)* **24**, 636 (1935).
- ³¹Th. Dittrich, M. Schartzkopff, E. Hartmann, and J. Rappich, *Surf. Sci.* **437**, 154 (1999).
- ³²S. Rauscher, Th. Dittrich, M. Aggour, J. Rappich, H. Flietner, and H. J. Lewerenz, *Appl. Phys. Lett.* **66**, 3018 (1995).
- ³³P. M. Lenahan, *Microelectron. Eng.* **22**, 129 (1993) and references therein.
- ³⁴J. Kočka, *J. Non-Cryst. Solids* **90**, 91 (1987), and references therein.
- ³⁵V. F. Kiselev and O. V. Krylov, *Electronic Phenomena in Adsorption and Catalysis on Semiconductors and Dielectrics* (Springer, Berlin, 1987).
- ³⁶C. Zener, *Proc. R. Soc. London Ser. A* **145**, 523 (1934).
- ³⁷E. A. Lebedev, E. A. Smorgonskaya, and G. Polisski, *Phys. Rev. B* **57**, 14 607 (1998).
- ³⁸J.-N. Chazalviel, F. Ozanam, and V. M. Dubin, *J. Phys. I* **4**, 1325 (1994).
- ³⁹A. O. E. Animalu, *Intermediate Quantum Theory of Crystalline Solids* (Prentice-Hall, Englewood Cliffs, New Jersey, 1977).
- ⁴⁰If the compensation is completely absent the increase of p with temperature can be much stronger than that given by the expression (3). For low temperatures one should expect $p \sim \exp(-E_p/2kT)$.